

## Supporting information

### **Hippuric acid–appended aminothiazole derivatives as ion-responsive metallogelators for visual detection of Ce(III)**

Priyanka Yadav<sup>a\*</sup> Mahammdmahir M. Saiyed<sup>a</sup> and Vinay S. Sharma<sup>b</sup>

<sup>a</sup>Department of Chemistry, Sardar Patel University, Vallabh Vidyanagar, Anand, 388120 Gujarat, India.

<sup>b</sup>Department of Chemistry, Parul institute of applied science, research and development cell, Parul university, Vadodara, Gujarat, 391760, India.

#### **Materials.**

All reagent grade materials were purchased from Sigma-Aldrich and used as received. The solvents used for the preparation of gels were purified, dried and distilled as required.

#### **Instrumentation.**

**FTIR spectroscopy:** FTIR Spectra were recorded on a Bruker –ALPHA II, FTIR instrument. Solid samples were recorded as an intimate mixture with powdered KBr.

**NMR spectroscopy:** The <sup>1</sup>H- NMR spectra were measured by using a Bruker AVANCE, 400MHz for <sup>1</sup>H-NMR with TMS as internal standard and CDCl<sub>3</sub>/DMSO as solvent.

**Scanning Electron Microscopic Study:** Morphologies of all reported gel materials were investigated using scanning electron microscopy (SEM). For SEM study, solution of a gelator is placed on a SEM sample holder and allowed to form gel, which was then dried under vacuum to give xerogel, and then the micrographs were taken in a SEM apparatus (FEI Nova NanoSEM 450 microscope)

**Rheometer.** The rheological experiments were carried out with a Anton paar - MCR102 Rheometer with a parallel plate configuration.

**X-ray Photoelectron Spectroscopy (XPS).** The XPS study were carried out with Thermo Scientific K-Alpha class or equivalent.

**Table S1. Comparison of Ce<sup>3+</sup> detection methods**

<b>Method</b>	<b>Detection Principle</b>	<b>Detection Limit (LOD)</b>	<b>Linear Range</b>	<b>Practicality/ Application</b>	<b>Trade-off Highlighted</b>
ICP-MS <sup>1</sup>	Mass spectrometry of ions		Wide (ppb–ppm)	Highly sensitive, precise	Requires expensive instrumentation, trained personnel
UV-Vis Spectroscopy <sup>2</sup>	Absorbance of Ce <sup>3+</sup> complexes	~0.1–1 ppm	ppm range	Moderate sensitivity, lab-based	Needs sample preparation, less portable
Electrochemical Sensors <sup>3</sup>	Redox response of Ce <sup>3+</sup>	~0.01–0.1 ppm	ppm range	Sensitive, portable options	Requires calibration, interference possible
Fluorescence Probes <sup>4</sup>	Quenching/enhancement by Ce <sup>3+</sup>	~0.1 ppm	ppm range	Sensitive, selective	Probe synthesis, stability issues
Thiazole-based Metallogel (this work)	Visual gel formation (qualitative)	~1000 ppm	Not established	Rapid, on-site, simple screening	Low sensitivity; suitable for highly contaminated samples

**Table S2- <sup>1</sup>H and <sup>13</sup>C NMR chemical shift changes of ligand 2a upon complexation with Ce<sup>3+</sup> ion.**

<b>Proton/Carbon Type</b>	<b>Free Ligand (ppm)</b>	<b>Metal Complex (ppm)</b>	<b>Typical Shift Direction</b>	<b>Reason</b>
Methyl protons (C-4)	2.00	2.05	Slight downfield	Inductive deshielding, minor effect.
CH <sub>2</sub> (Near carboxylic group)	3.90	4.14	Downfield	deshielding and line broadening
NH of amide group	8.81	9.02	Downfield	deshielding and line broadening
-CH of thiozole ring	6.06	6.10	Slight downfield	deshielding, minor effect.
-CH benzene ring near to amide group	7.84	7.91	Slight downfield	deshielding, minor effect.
Carbon of carboxylic group (C=O)	171.46	172.49	Downfield	Direct coordination site →strong deshielding.
carbon attached to NH <sub>2</sub> and ring N-atom	168.33	168.77	Slight downfield	π-electron withdrawal by metal center.
Carbon of amide group attached to aromatic ring	166.09	167.01	Downfield	Direct coordination site →strong deshielding.
Carbon attached to ring sulphur atome (C-S)	100.10	101.156	Downfield	site for hydrogen bonding →strong deshielding.

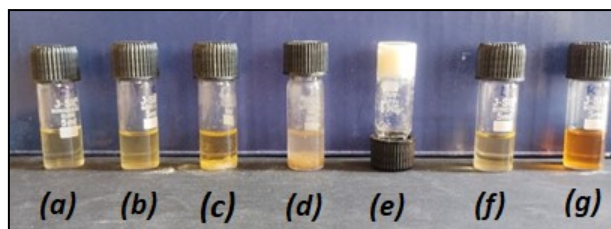


**Fig.S1** photograph of ion selective response of ligand 2a with (a)  $Zn^{2+}$ , (b)  $Cd^{2+}$ , (c)  $Pb^{2+}$ , (d)  $Ag^+$ , (e)  $Ce^{3+}$ , (f)  $Li^+$ , and (g)  $K^+$

### Analytical data

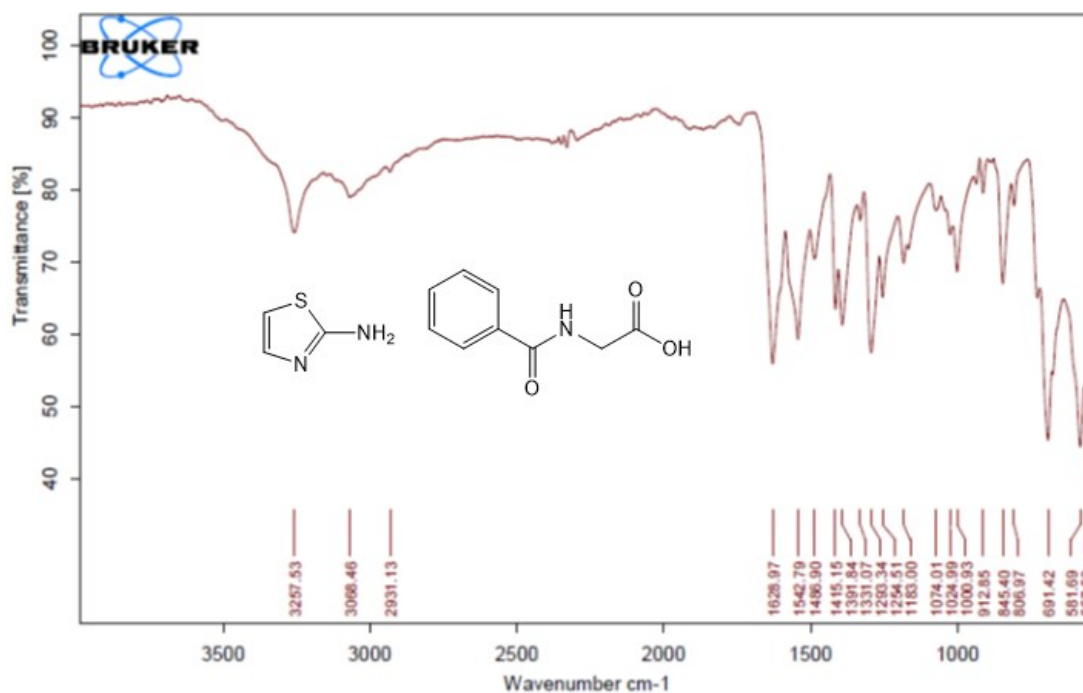


**Fig.S2** IR spectra of compound-1a.

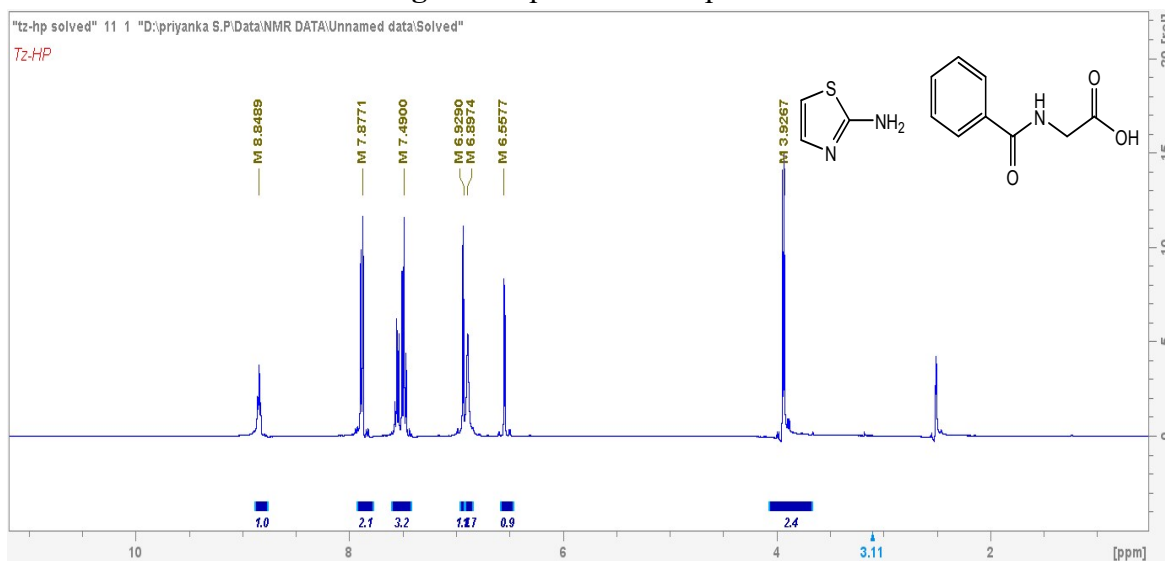


**Fig.S3**  $^1H$ NMR spectra of compound-1a.

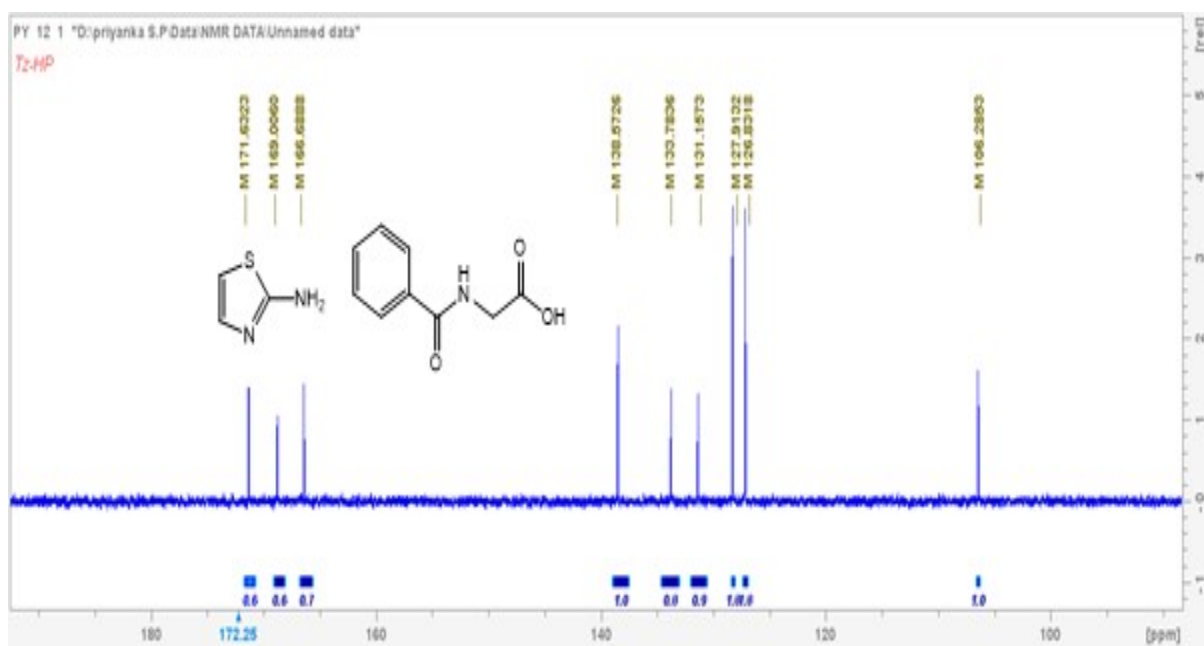


Fig.S4 <sup>13</sup>CNMR spectra of compound-1a.

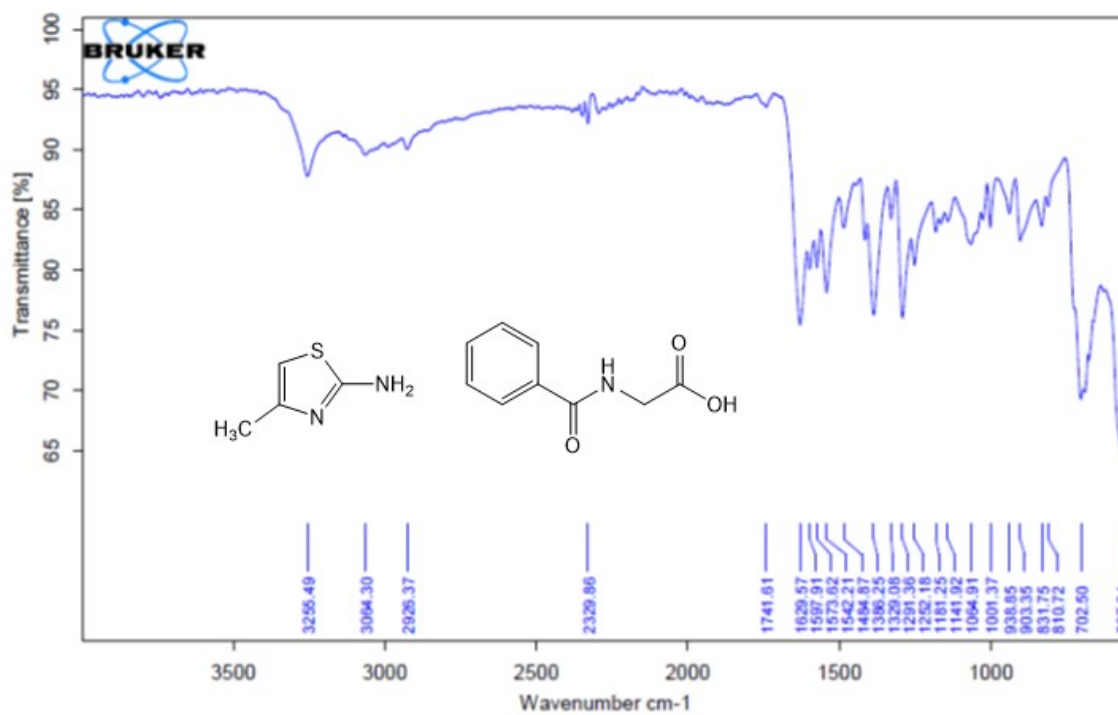


Fig.S5 IR spectra of compound-2a.

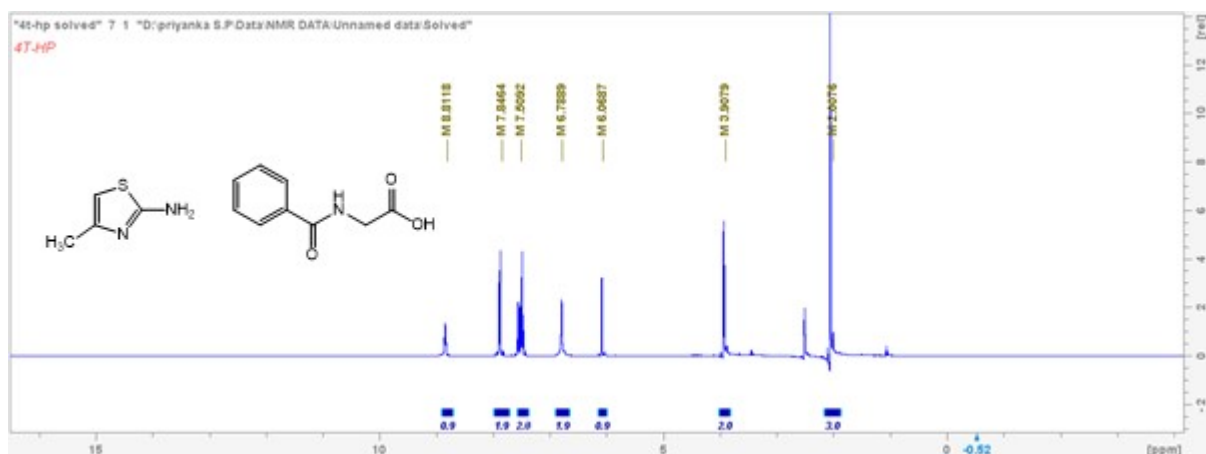


Fig.S6 <sup>1</sup>H NMR spectra of compound-2a.



Fig.S7 <sup>13</sup>C NMR spectra of compound-2a.

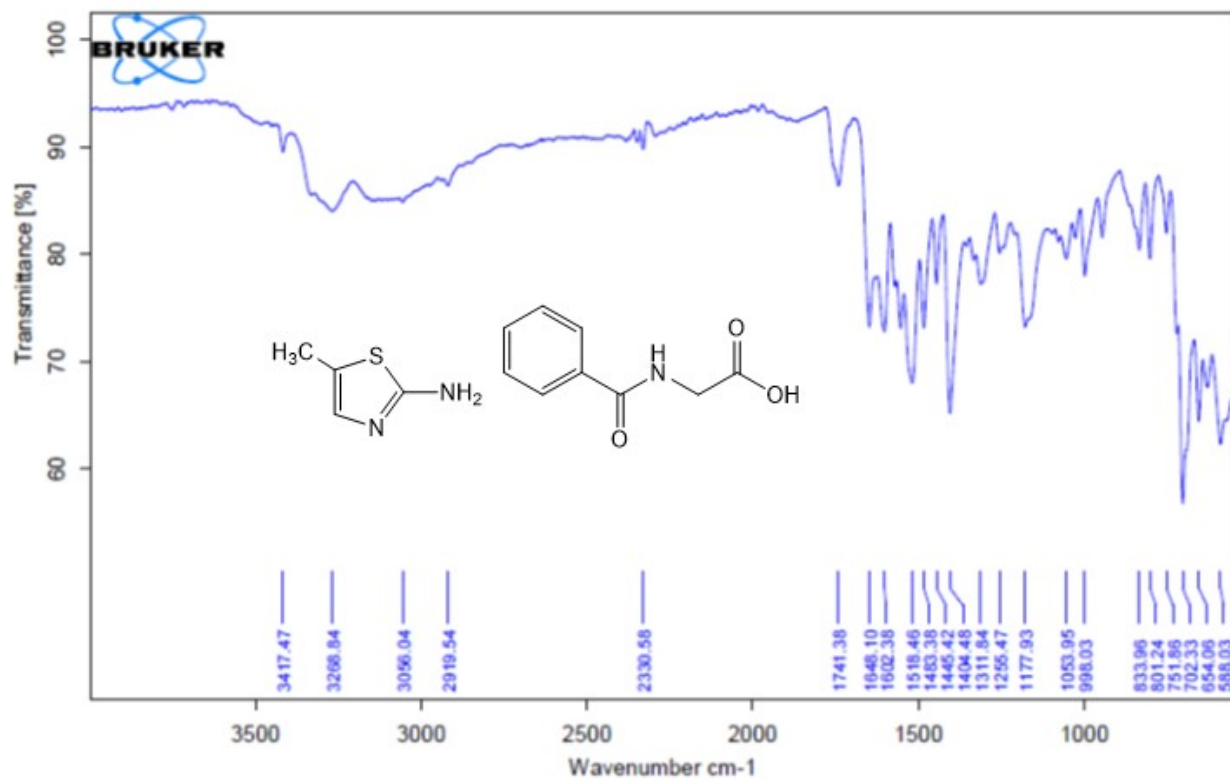


Fig.S8 IR spectra of compound-3a

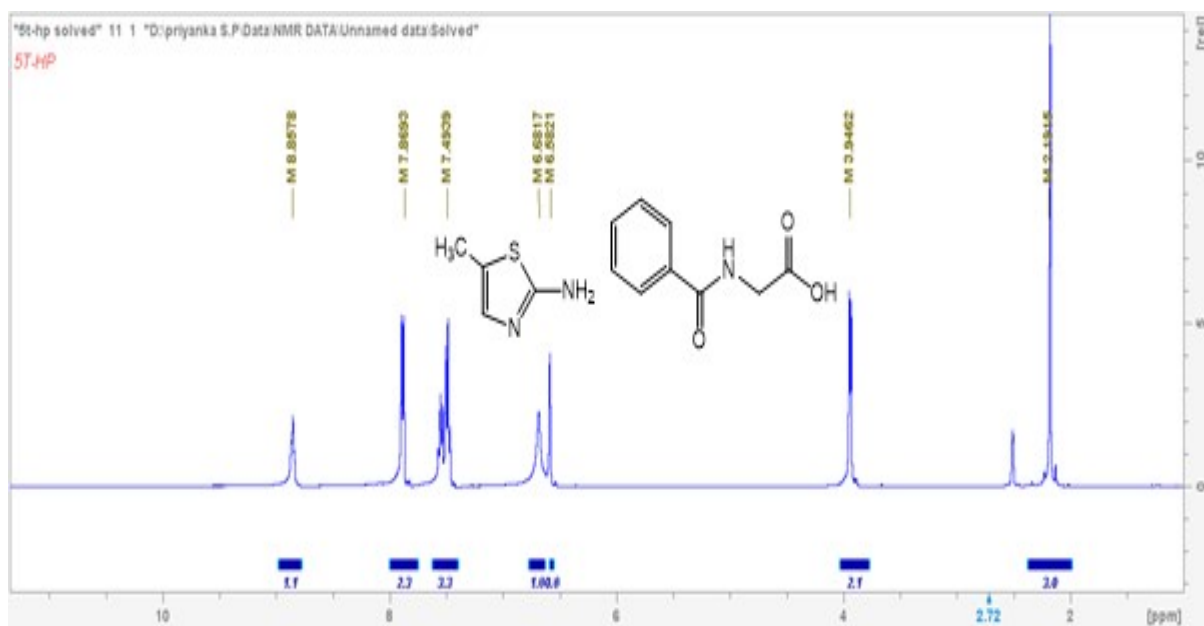


Fig.S9 <sup>1</sup>H NMR spectra of compound-3a.



Fig.S10 <sup>13</sup>C NMR spectra of compound-3a.

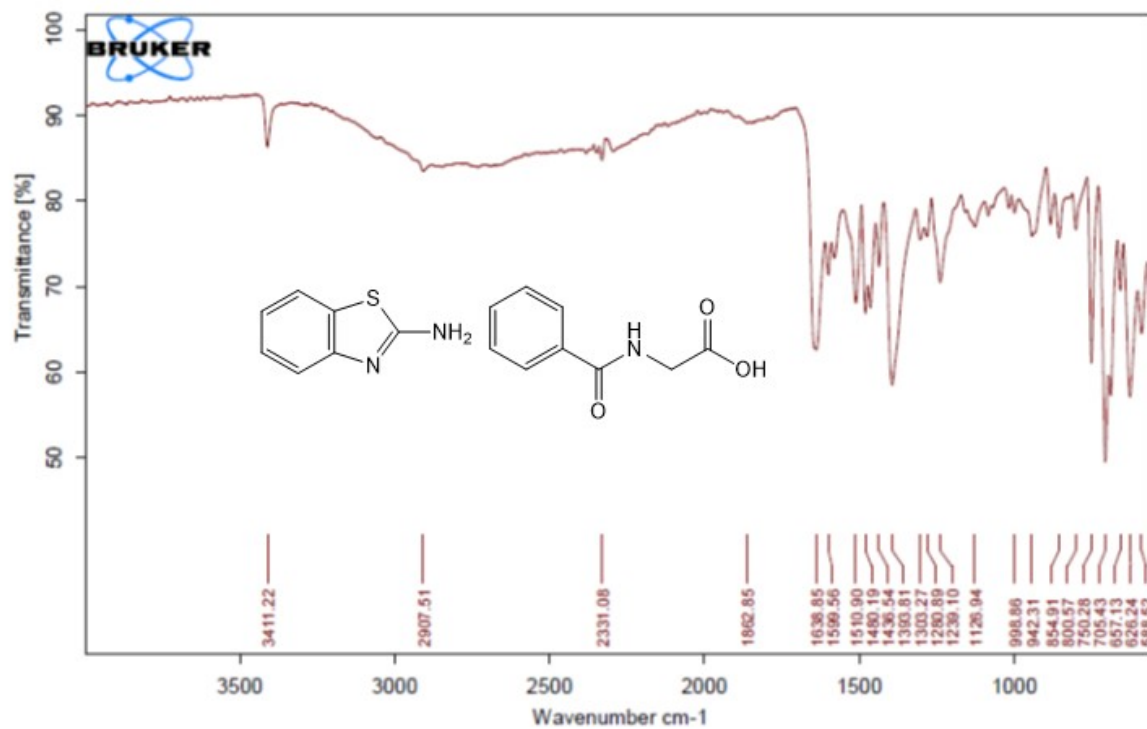


Fig.S11 IR spectra of compound-4a

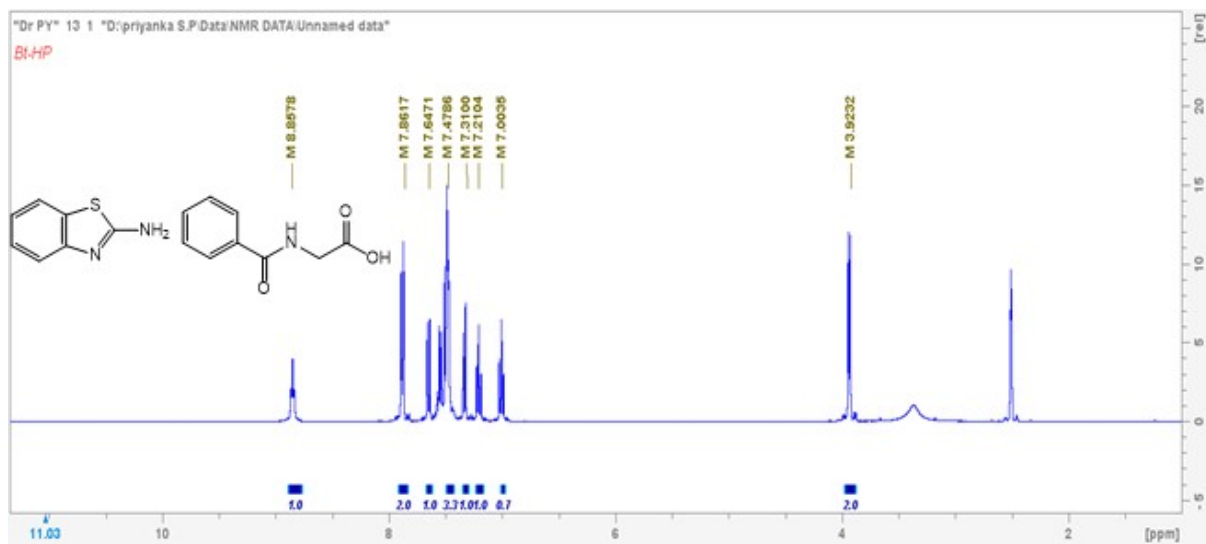


Fig.S12 <sup>1</sup>H NMR spectra of compound-4a.

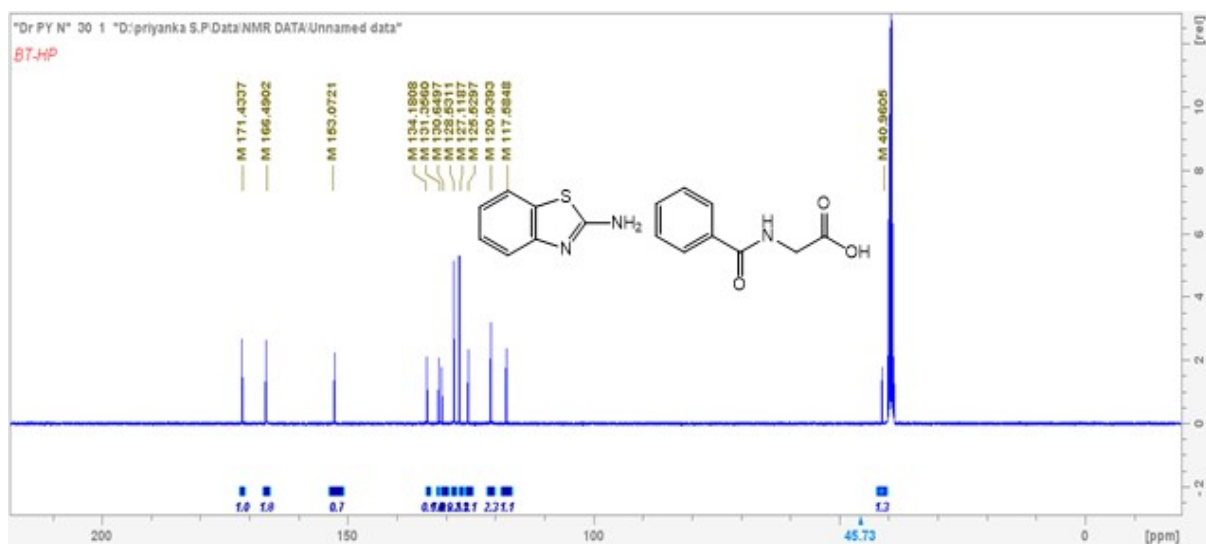


Fig.S13  $^{13}\text{C}$  NMR spectra of compound-4a.

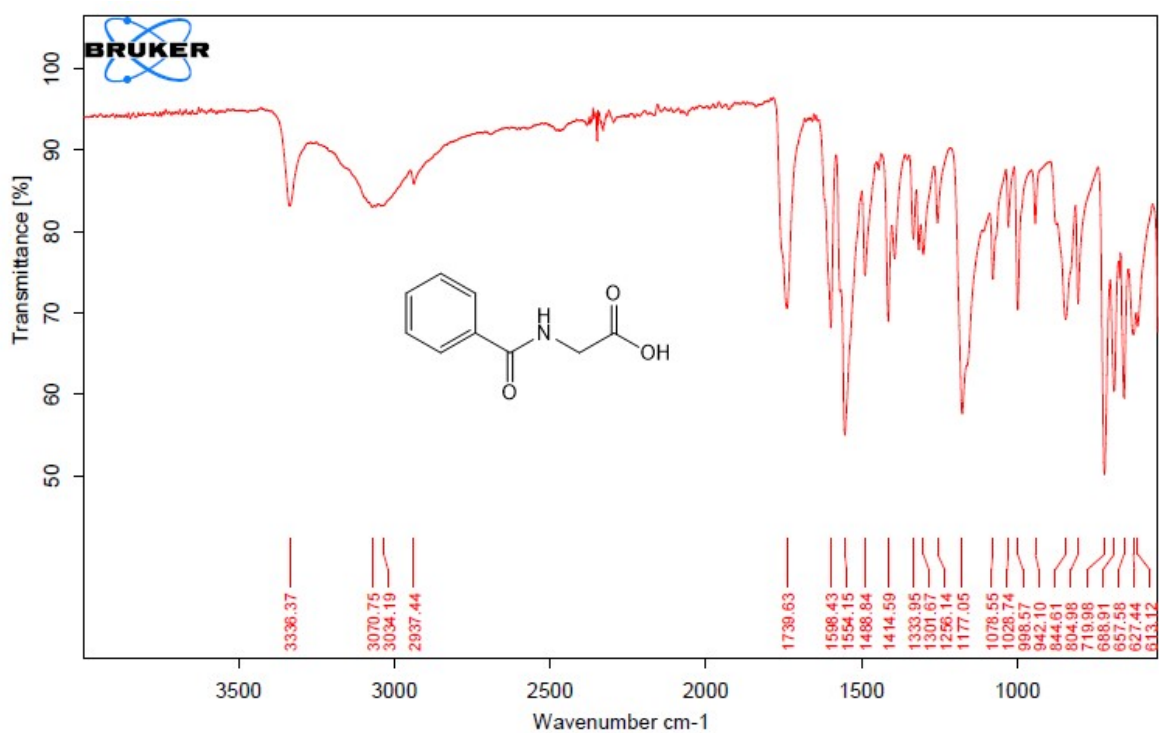


Fig.S14 IR spectra of hippuric acid compound-a.

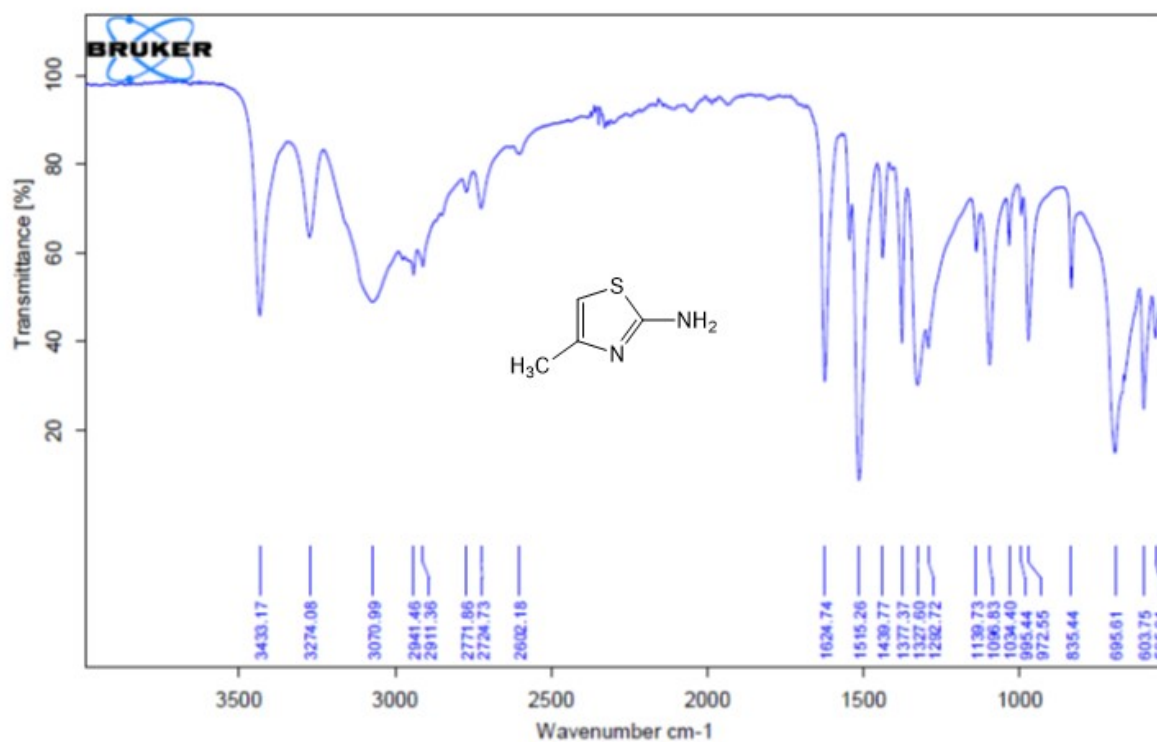


Fig.S15 IR spectra of 2-amino-4-methylthiazole compound-2.

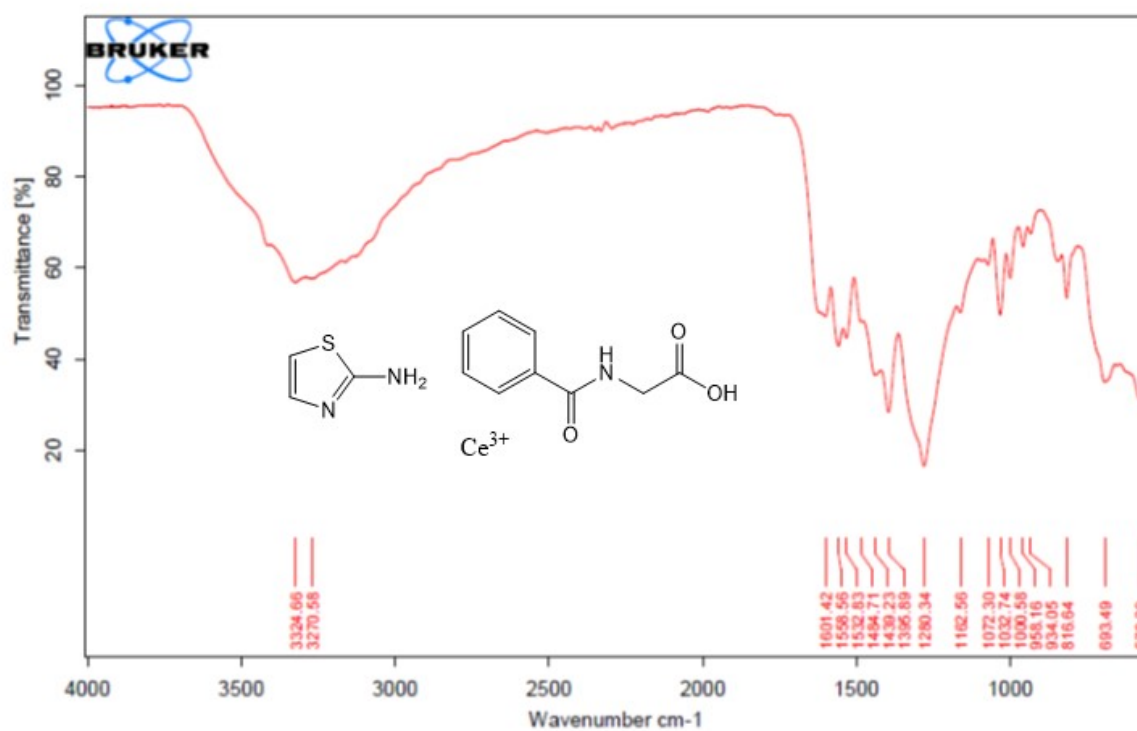
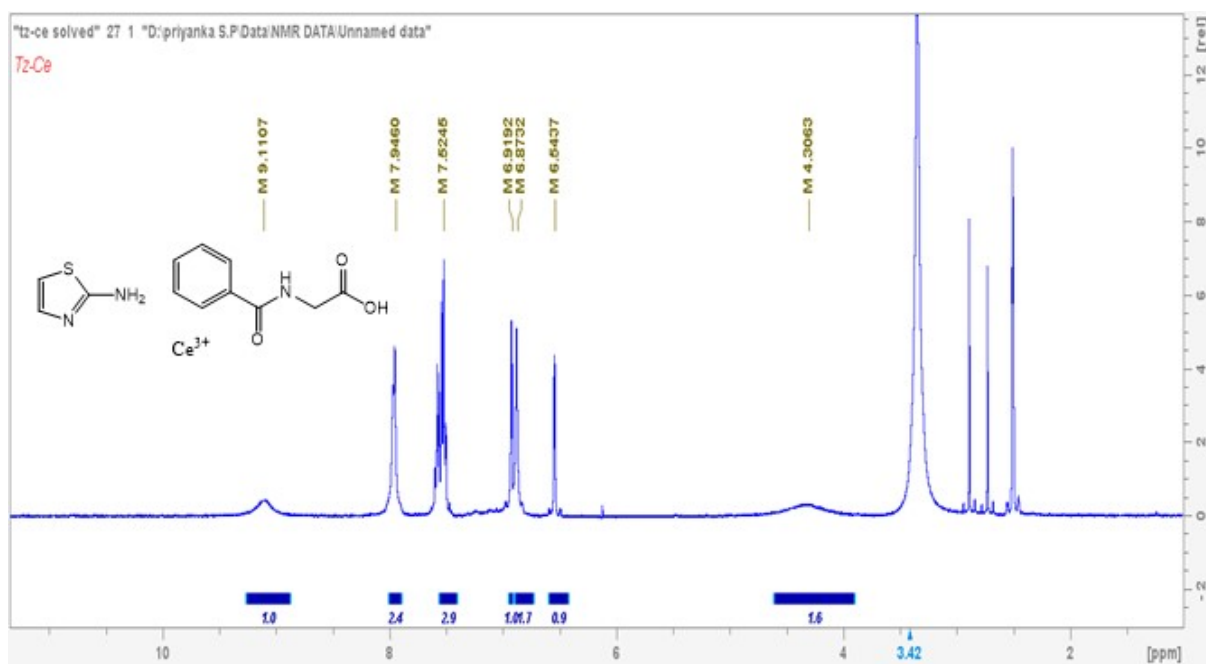
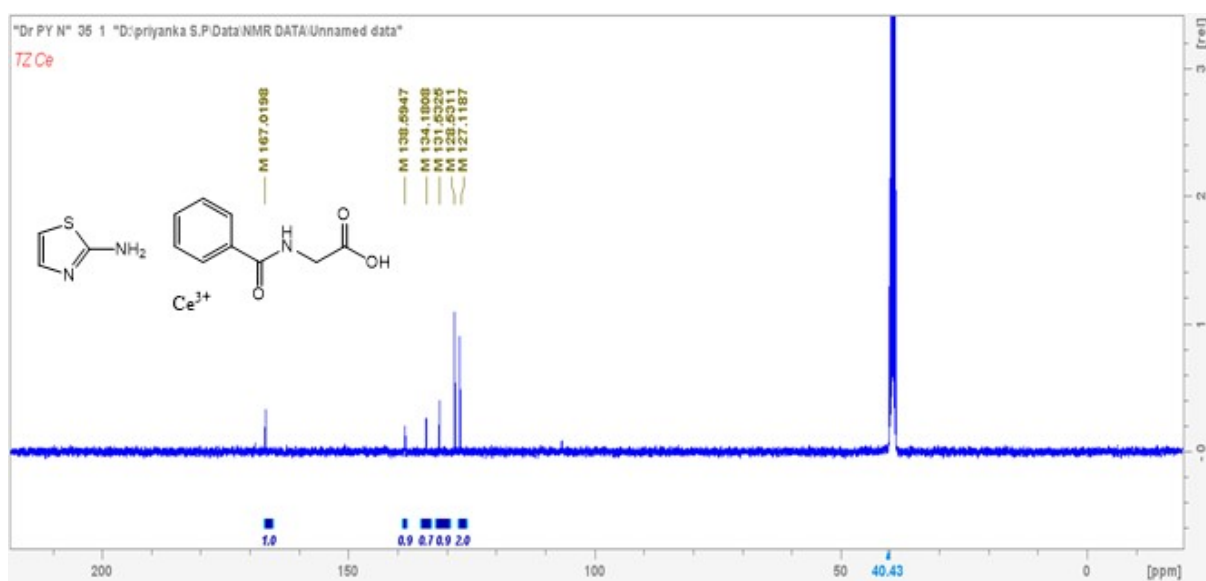


Fig.S16 IR spectra of 1a-Ce.



**Fig.S17**  $^1\text{H}$ NMR spectra of compound-1a-Ce.



**Fig.S18**  $^{13}\text{C}$  NMR spectra of compound-1a-Ce.

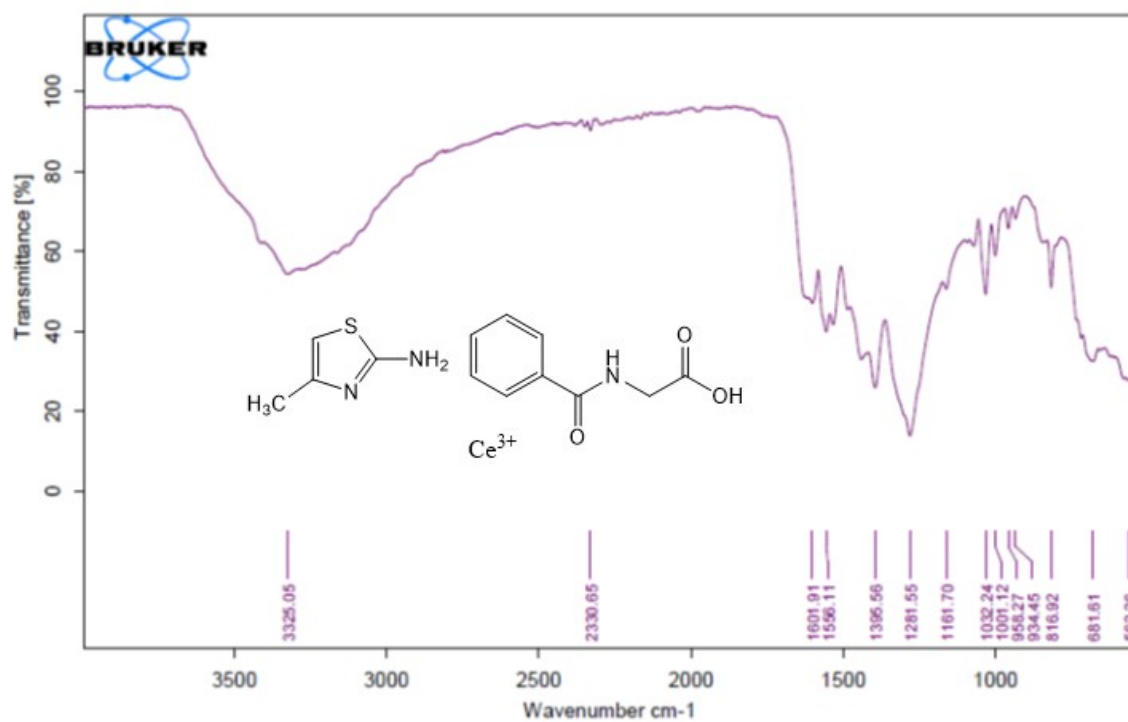


Fig.S19 IR spectra of compound-2a-Ce

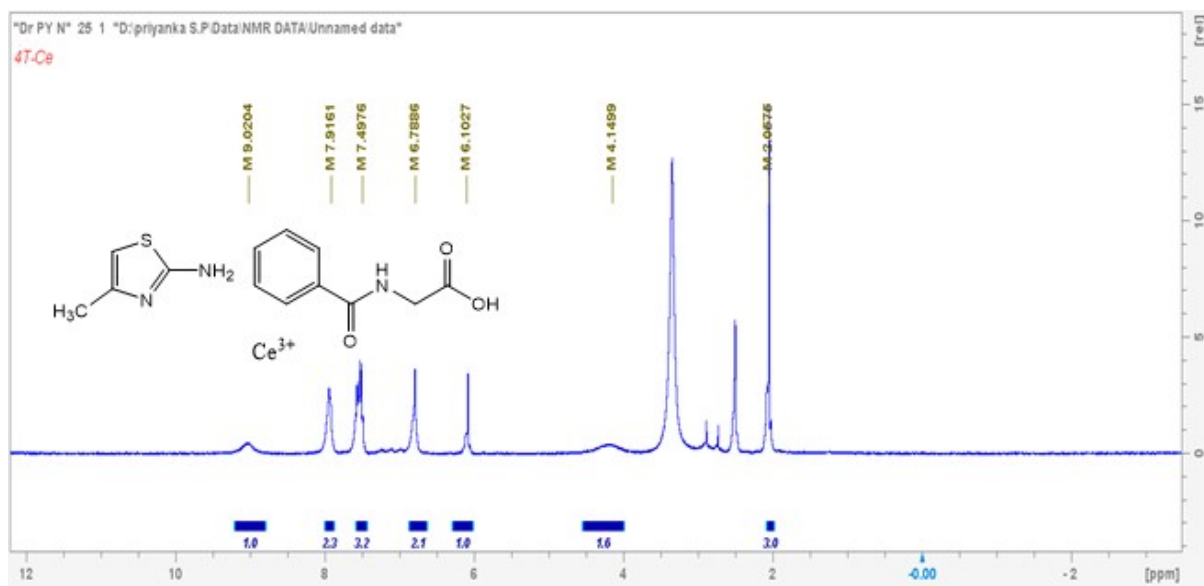


Fig.S20 <sup>1</sup>H NMR spectra of compound-2a-Ce.

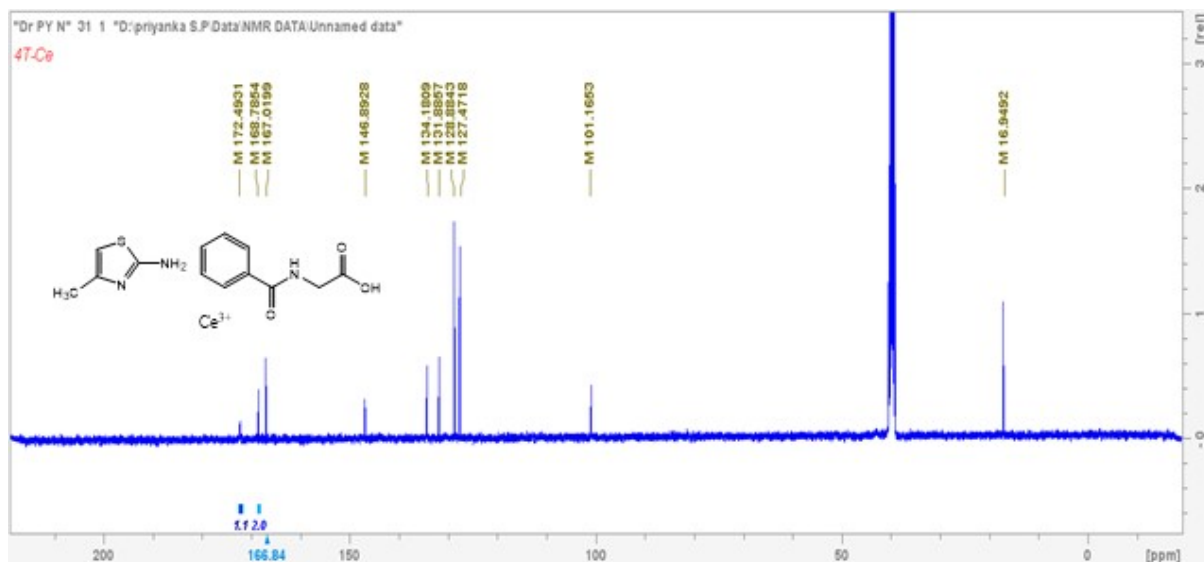


Fig.S21  $^{13}C$ NMR spectra of compound-2a-Ce.

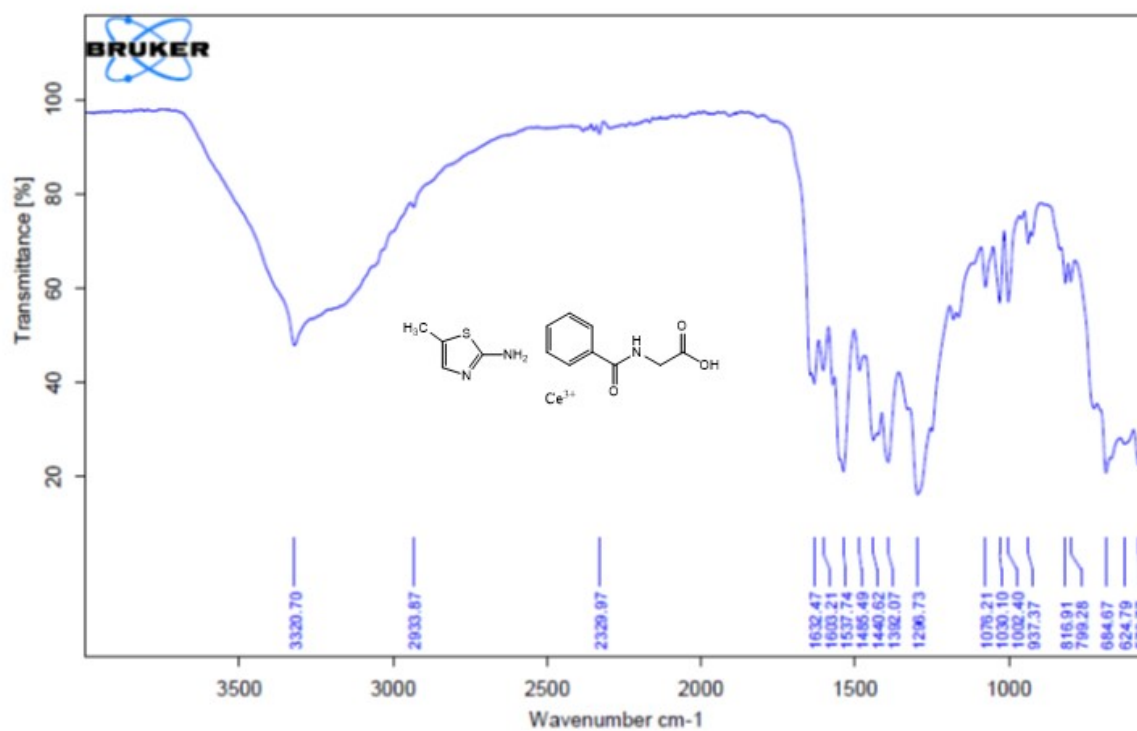


Fig.S22 IR spectra of compound-3a-Ce

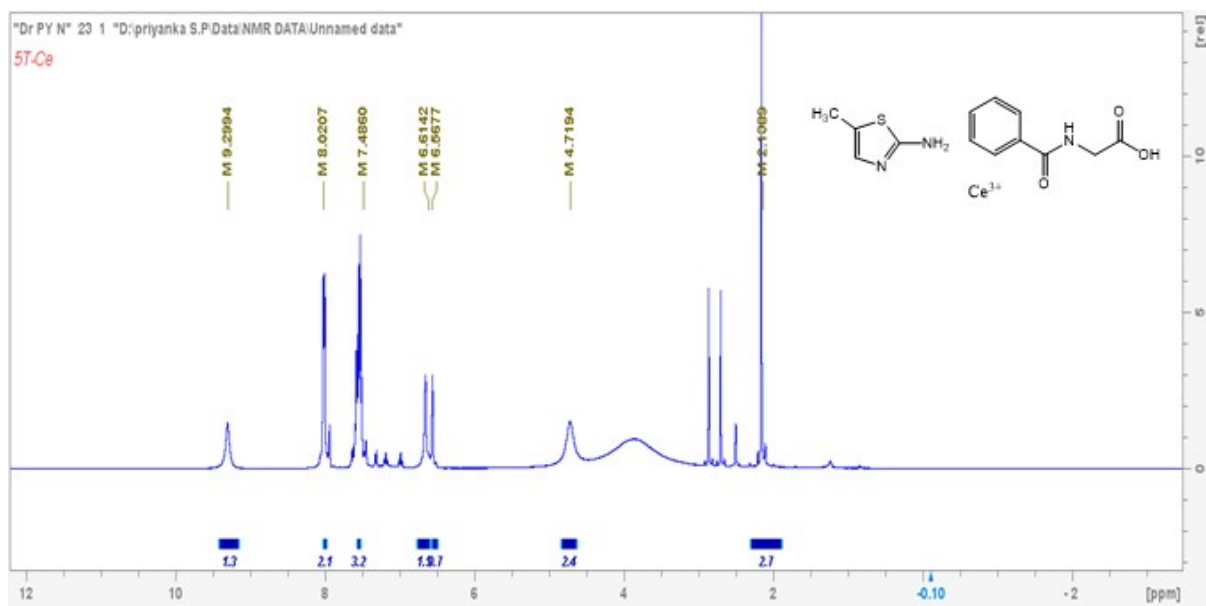


Fig.S23  $^1H$ NMR spectra of compound-3a-Ce

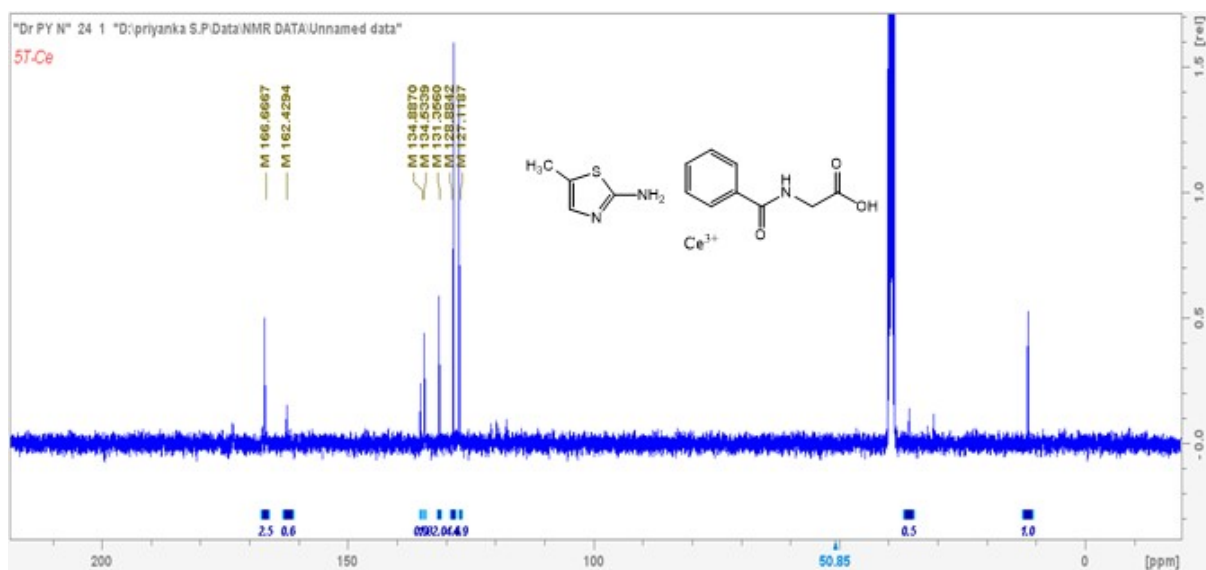


Fig.S24  $^{13}C$ NMR spectra of compound-3a-Ce.

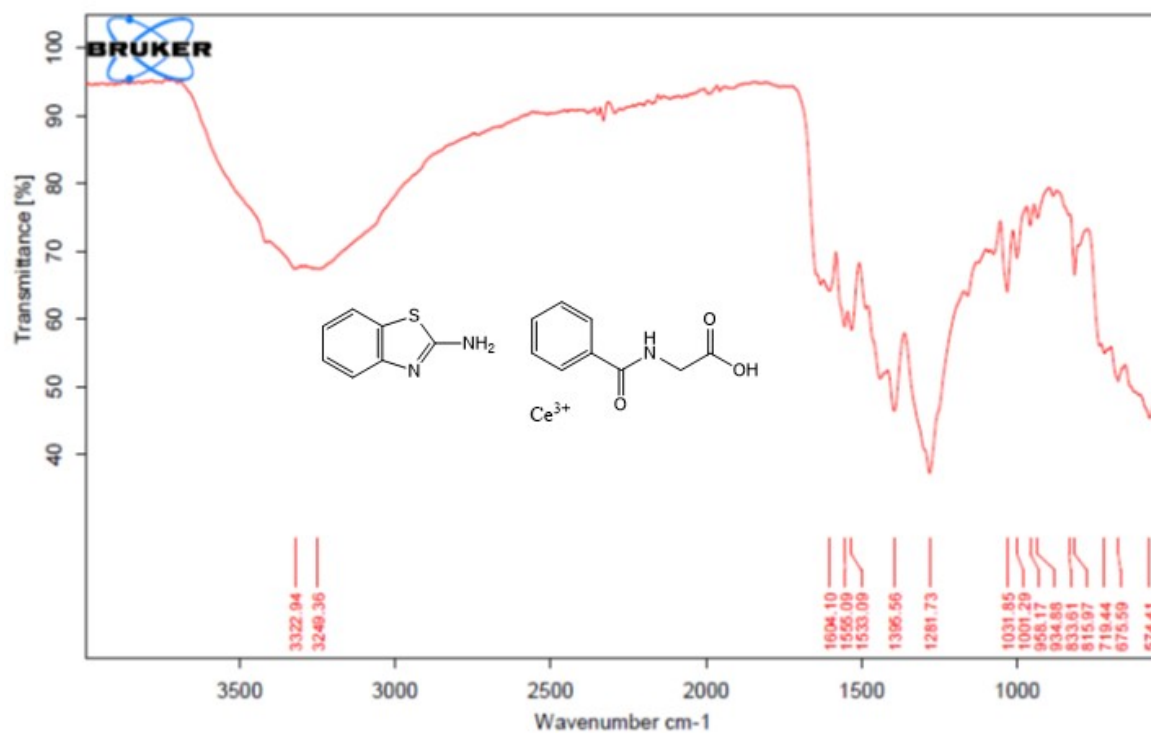


Fig.S25 IR spectra of compound-4a-Ce

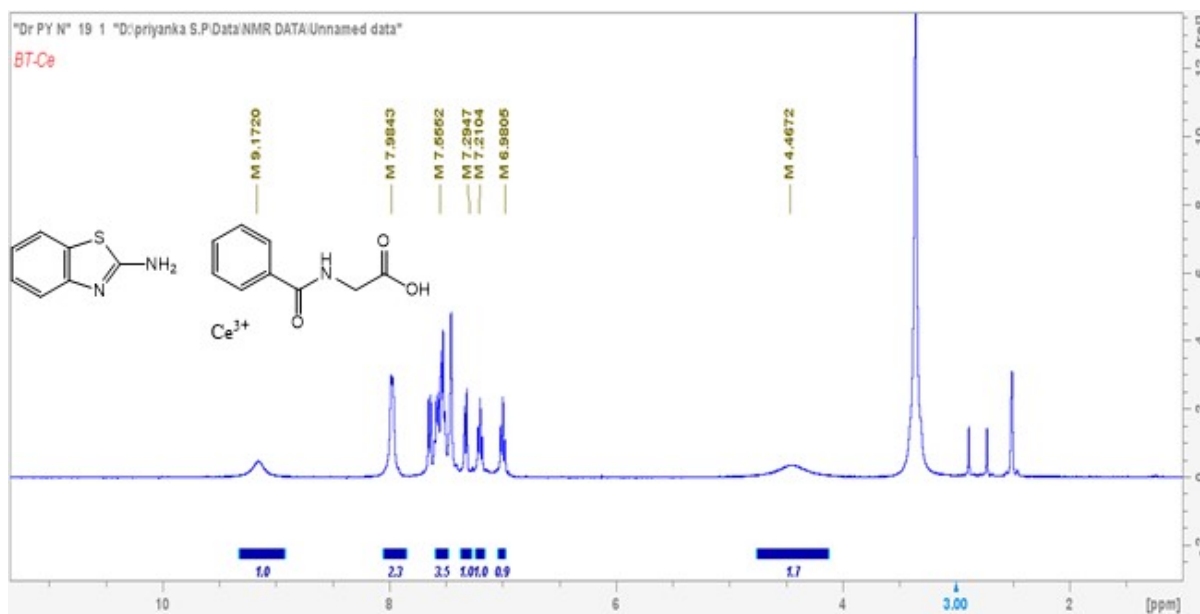
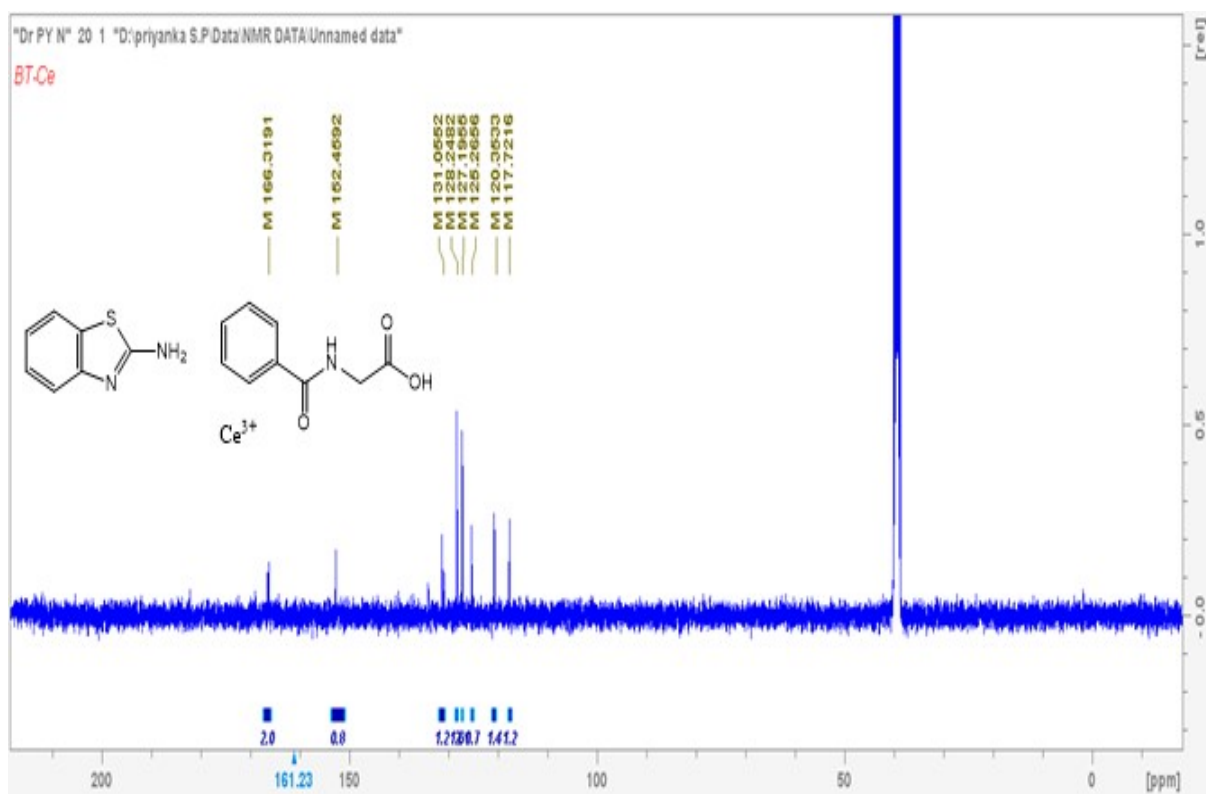
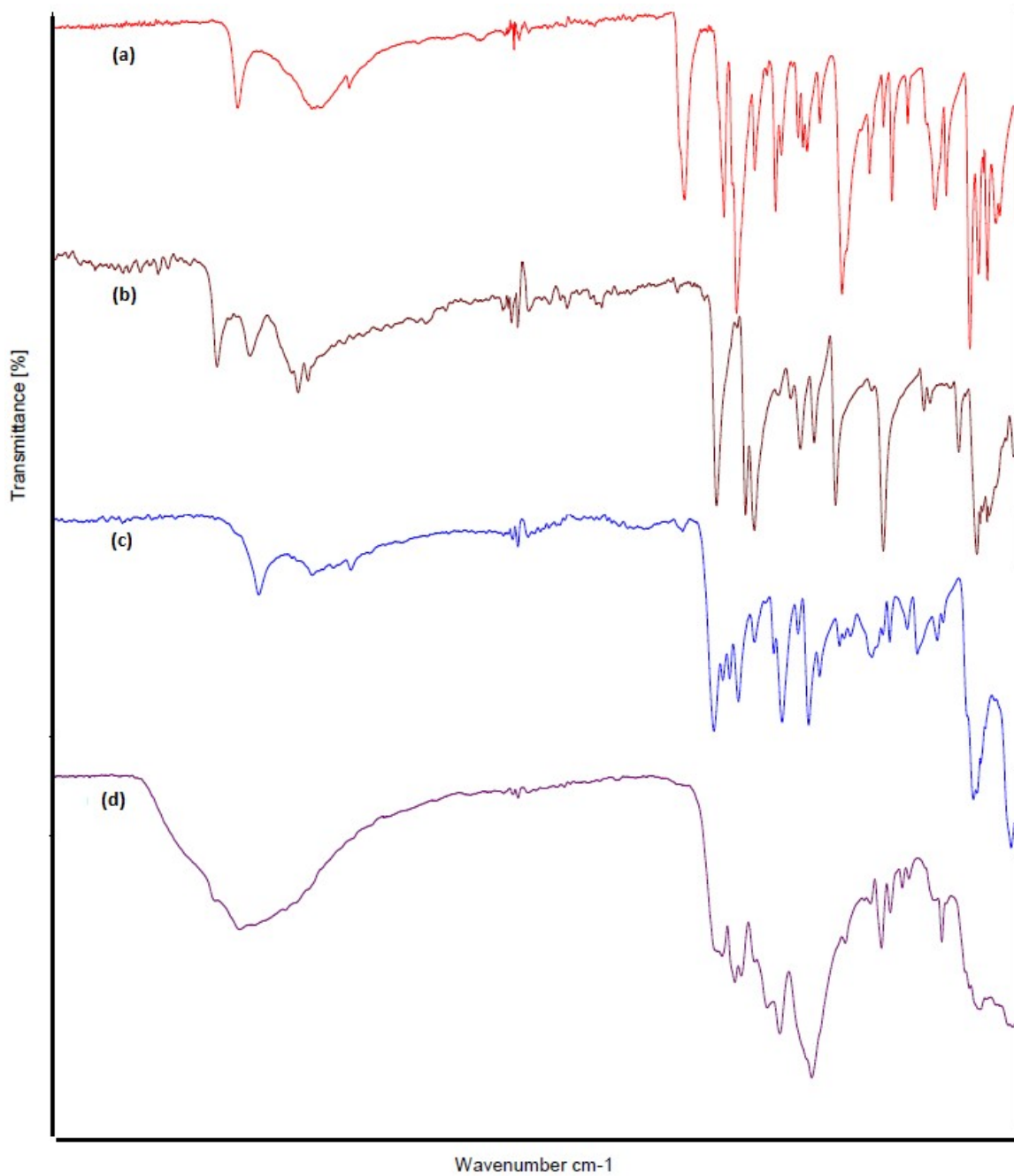


Fig.S26 <sup>1</sup>H NMR spectra of compound-4a-Ce



**Fig.S27**  $^{13}\text{C}$ NMR spectra of compound-4a-Ce.



**Fig.S28** Overlapping IR spectra of (a) Compound-a, (b) Compound-2, (c) Compound-2a, and (d) Compound-2a-Ce. The spectra illustrate the progressive changes in vibrational features upon structural modification and Ce<sup>3+</sup> incorporation.

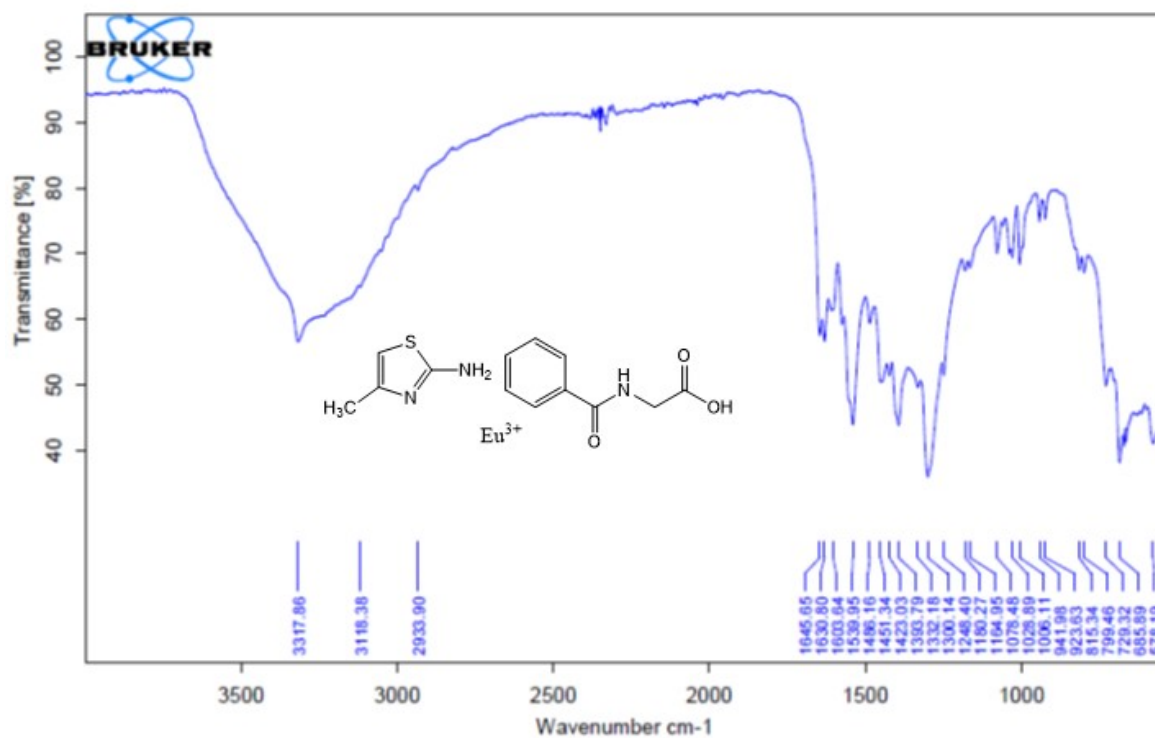


Fig.S29 IR spectra of compound-2a-Eu<sup>3+</sup>

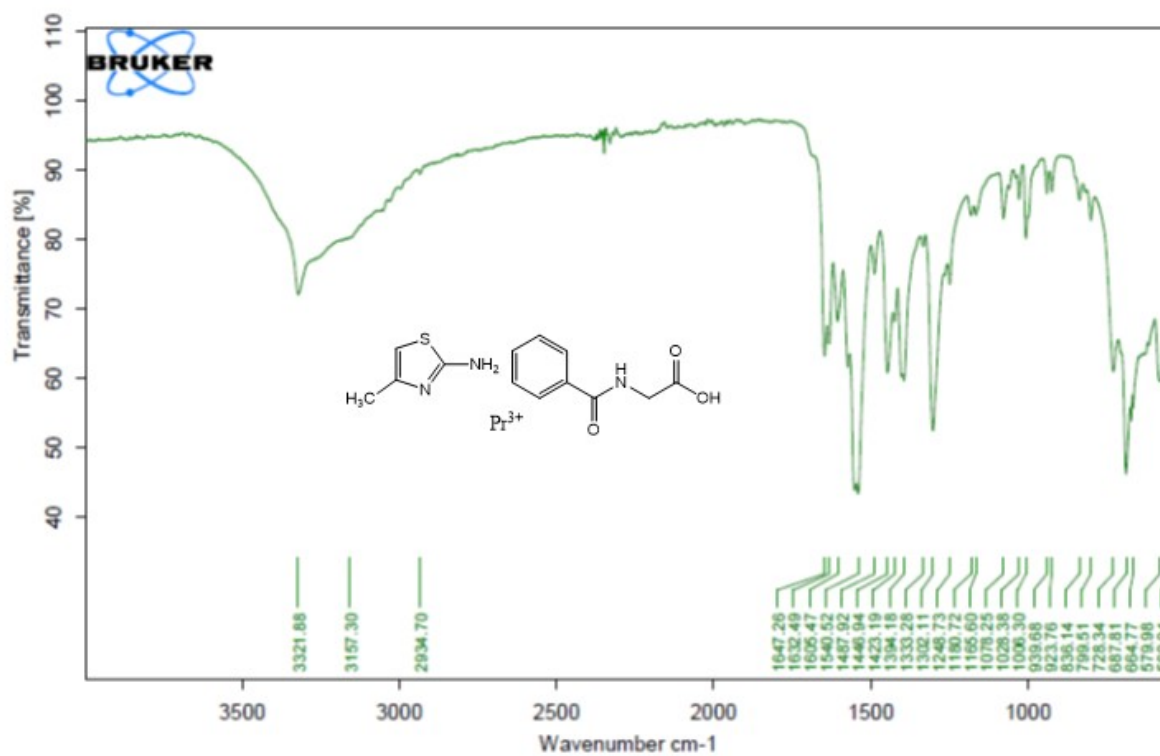


Fig.S30 IR spectra of compound-2a-Pr<sup>3+</sup>

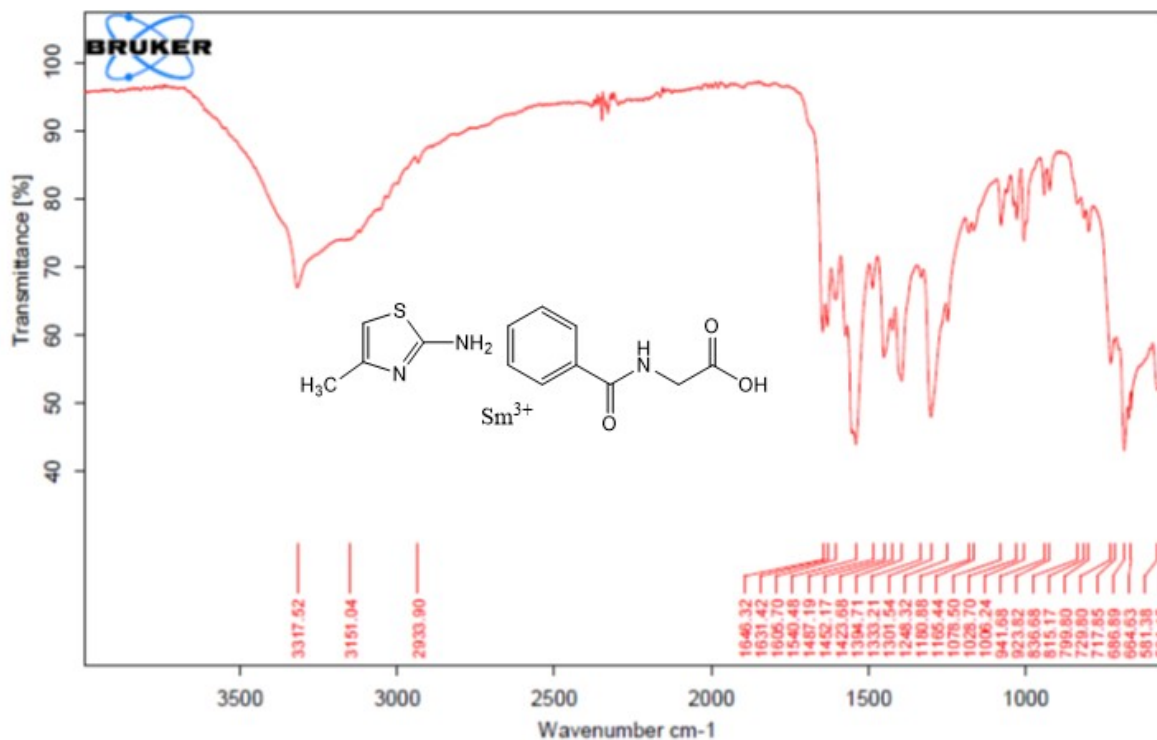


Fig.S31 IR spectra of compound-2a-Sm<sup>3+</sup>

## References

1. Y. Hua, ICP-MS determination of trace Ce(III) in environmental samples, *Anal. Methods*, **2021**, *13*, 4567–4574.
2. Quinoline-based probes for fluorescent and electrochemical sensing of Ce<sup>3+</sup>, *J. Photochem. Photobiol. A: Chem.*, **2020**, *400*, 112706.
3. X. Luo, Spiropyran fluorescent probe for Ce<sup>3+</sup> detection, *J. Rare Earths*, **2020**, *38*, 1234–1242.
4. Bio-inspired nanochannel/membrane for Ce<sup>3+</sup> detection in wastewater, *Chem. Eng. J.*, **2023**, *456*, 132145.